Science Justification

Motivation: Continuation of the Legacy, Design for the Future

Dust plays a significant role during the star formation process by enhancing the formation of molecular hydrogen (H_2) and the shaping of the spectral energy distribution (SED) of galaxies by absorbing UV photons from stars and re-radiating the energy in the far-IR. To draw the full picture of cosmic star-formation history and to understand the physical drivers for galaxy evolution, it is necessary to investigate the properties of dust in galaxies at different epochs and determine the factors that drive cosmic dust evolution.

In the observed frame, the most critical window for studying dust is the rest-frame $> 100\,\mu$m, beyond the peak of the SED, i.e., in the Rayleigh-Jeans wavelength range. Numerous dusty star-forming galaxies (DSFGs) selected in the far-IR/submillimeter are identified to be relatively massive ($> 10^{10}\,M_\odot$) galaxies with high star-formation rates (up to few hundreds $M_\odot\,yr^{-1}$) at redshifts $1 < z < 3$ (Hodge et al. 2013; Casey et al. 2014; da Cunha et al. 2015). Although their number density is much smaller than that of LBGs selected in the rest-frame optical, the large SFRs of these galaxies place DSFGs as the most extreme cases of star-forming galaxies in the Universe (Whitaker et al. 2017). The contribution to the global cosmic SFR density by DSFGs increases as we move to $z > 1$ (Le Floch et al. 2005; Magnelli et al. 2013) and the trend seems to remain for $z \sim 3$. However at $z > 3$, the volume number density of DSFGs is relatively unconstrained (Casey et al. 2018) and thus it is not clear what stage in galaxy evolution is represented by DSFGs. As more detections have been made of $z > 4$ LBGs in ALMA bands, our knowledge on the dust attenuation and ISM properties of normal/typical star-forming galaxies in the early Universe has been increasing (Willott et al. 2015; Smit et al. 2017; Bowler et al. 2018). Nevertheless, numbers of non-detections for the dust continuum have also been reported (Bouwens et al. 2016; Inoue et al. 2016; Carniani et al. 2018), suggesting a diversity of dust properties between different galaxies.

The modelling of dust emission in galaxies requires us to study the factors that affect dust properties, e.g., dust mass, grain-size distribution and metallicity, which are currently limited only to the local Universe. The existence of supermassive black holes in the centers of galaxies affects the dust emission through heating, thus the co-evolution of AGN and galaxies needs to be considered in the study of dust evolution. All these unresolved issues can be addressed through multi-wavelength (mid-IR and far-IR being the most critical) surveys of deep fields.

The North Ecliptic Pole (NEP) is one of the most frequently visited areas of the sky because of its easy accessibility for space missions. In addition to the currently available multi-wavelength data sets over few deg^2 regions around the NEP (mostly based on *AKARI*'s legacy multi-wavelength surveys from UV to mid-infrared; e.g., Matsuhara et al. 2006; White et al. 2010; Takagi et al. 2012; Kim et al. 2012; Oi et al. 2014; see Fig. 1), a number of upcoming space-based surveys have marked this region as one of the most advantageous fields to address questions regarding the cosmic evolution of dust in galaxies. The X-ray telescope *eROSITA* will carry out an all-sky survey with the goal of finding rare populations of heavily dust-obscured AGN, while having the longest total exposure in the NEP region. *Euclid*, a space-based mission to map the dark matter distribution of the Universe based on weak-lensing and precise redshift measurements, will also target the NEP as one of the three "*Euclid*-deep" fields to study numerous topics related to galaxy evolution. *SPHEREx*, an all-sky spectral survey mission in the near-IR is another approved project that will provide a high cadence, deep survey in the NEP region. Both *Euclid* and *SPHEREx* will provide low spectral resolution spectra in the near-IR for most, if not all, *AKARI* near-IR selected extragalactic objects as early as 2023. **We expect near-IR spectral information will be of particular use when combined with far-IR to submm surveys over a wide area** to sample the high-z DSFG population.

The *Herschel*/SPIRE 250, 350, 500 μm survey over the NEP is rather shallow and suffers from the poor spatial resolution of the *Herschel*. However, SCUBA-2 850 μm data obtained during the last few years has been much better than *Herschel*/SPIRE in identifying *AKARI* near-IR selected galaxies in the far-IR (Seo et al. 2018). Before the advent of the next-generation mapping instruments with enhanced mapping speeds (such as TolTEC on the LMT), SCUBA-2 remains one of the most efficient mapping instruments for obtaining information at the Rayleigh-Jeans limit of galaxies.

As a way of preparing for upcoming visible-to-near-IR surveys, we need **to complete the previous large NEP program, NEPSC2-Wide (M17BL007), which is currently only half completed**. In addition to that, to maximally exploit the scientific merits of the 850-μm data, we request **to obtain "deeper" 850-μm data that matches with other planned surveys: NEPSC2-Deep**. The key science questions our new large program will address are: *(i) How abundant were DSFGs in the early Universe, and what are the dust properties of LBGs at $z > 6$? (ii) Are the dust scaling relations (dust mass function, dust-to-gas ratio, and dust-to-metal ratio) of $z > 1$ galaxies consistent with those of local galaxies, and what parameters determine the dust properties of galaxies? (iii) What portion of the IR luminosities of obscured AGN is powered by star formation?* Answering these questions will need **a wide far-IR/submm survey, preferentially multi-colored** to break degeneracies in constraining dust masses with different dust temperatures and grain-size distributions.

Key Science 1: Dusty Galaxies in the Era of Reionization

Recent discoveries of dusty star-forming galaxies at $z > 6$ suggest that such previously-missed galaxy populations comprise a significant portion of the early galaxy population (e.g., Watson et al. 2015; Laporte et al. 2017; Zavala et al. 2018; Tamura et al. 2019; Wang et al. 2019). The large dust masses (few times $10^6 M_\odot$) and young stellar ages (few Myrs) of these galaxies challenge existing dust evolution models (Lesniewska & Michalowski 2019). Cosmological zoom-in simulations and dust radiative-transfer models reproduce the massive dusty galaxies (Pallottini et al. 2019), but to reproduce *normal* galaxies the required star-formation rate is a few times higher than naively estimated (Behrens et al. 2018) or alternatively the galaxies need to contain older stellar populations (Tamura et al. 2019). However, a number of discoveries have been made from the lensed galaxy population (albeit with intrinsic uncertainties in lensing factors), suggesting a global effect that dust temperatures (T_{dust}) based on the peak emission wavelength increase with redshift, in line with the specific star-formation rate increase at high z (Liang et al. 2019). The next generation of large surveys at mm wavelengths with large singie-dish millimeter observatories having large fields of view will help to construct a census of obscured galaxies at such early epochs.

Factors that limit the discovery and study of DSFGs at such early times include their (very rare) number density and the T_{dust}–z degeneracy. Firstly, unlike the far-UV luminosity function of LBGs, which is described by a steep faint-end slope and an exponential fall at the bright end (e.g., Bouwens et al. 2017), the far-IR luminosity function is often described as a broken double-power law (e.g., Patel et al. 2013; Wang et al. 2017). Thus the number of DSFGs would be much smaller than that of LBGs. A second factor is the limitation of FIR-to-submm colors. Negative K-correction is clearly a benefit for high-z galaxy selection, since at 850 μm the expected continuum flux density is almost constant from $z = 2$ to $z = 8$. However, because of this advantage, monochromatic submm continuum flux densities cannot constrain the redshift of detected sources. Therefore the best place to constrain this population is where ultra-deep infrared spectroscopy is imminent, i.e. in the deep *Euclid* field in the NEP, and where mm-wave redshift campaigns (LMT, NOEMA) are likely to be triggered and driven by mm-wave continuum surveys.

We are now facing the prospect of new instruments with faster mapping speed and better spatial resolution at > 1 mm. TolTEC, which will be commissioned on the 50-m single-dish Large Millimeter Telescope in 2020, is one such instrument planning a large (up to few tens of deg^2) survey with a depth of 0.2 mJy/beam rms. ~ 10 deg^2 around the NEP has been selected as a priority 1 survey field, and it is expected that we will eventually have 1.1, 1.4 and 2 mm data over the NEP to interesting depths.

The millimeter continuum fluxes and colors will allow us to select DSFG candidates at $z > 5$ with sample sizes as large as > 200 deg^{-2} (according to Cai et al. 2013 model). However, without 850 μm fluxes, $[1.1-1.4]$ mm and $[1.4-2]$ mm colors are not enough to constrain dust temperatures, i.e., total IR luminosity in these galaxies (see Fig. 2; Serjeant 2019). Since the NEP is the only *Euclid*-deep field among the priority 1 TolTEC fields, the validation of the selection method for DSFGs at $z > 6$ in a modest-sized SCUBA-2 850 μm field would guarantee the reliability of selected DSFGs at the reionization epoch. A diameter of 30 arcmin used in PONG1800 recipe roughly corresponds to $50h^{-1}$ Mpc at $z = 6$, comparable to a mean separation between present-day massive galaxy clusters. Therefore 0.5 deg diameter field is a scale of homogeneity in galaxy population studies. The ultra-high-z (sub)mm-wave population is well matched to that of *Euclid*: one PONG1800 area will have 10 TolTEC galaxies at $z > 6$ (and 41 at $z > 5$), and the same area will have 10–30

Lyα emitters at $z > 6.5$ in *Euclid* (plus more LBGs). The naive SFRs are quite different at a few $M_\odot$/yr with *Euclid* versus a few 100 in the (sub)mm, but this is without any rest-frame UV dust correction. We will measure or constrain dust temperatures and bolometric luminosities of known very high-z galaxies from TolTEC, determine their obscured/unobscured star-formation rate ratios, and compare the star-formation density fields for obscured and unobscured star formation in the same ultra-high-redshift comoving volume (also making us immune to cosmic-variance effects).

Key Science 2: Dust-to-Gas Ratio Variation in Galaxies

Star formation is the most important baryonic process in galaxy evolution, since it influences the morphological transition of galaxies and drives galaxy size build up. Our current picture of the cosmic star-formation history suggests that there has been a significant decrease after a peak of star formation at $z \simeq 2$–3. The rapid decline of the star formation since then is either due to the exhaustion of the cold gas or the decline of the star-formation efficiency, which would only be distinguished with the knowledge of the molecular gas in the high-redshift star-forming galaxies.

Measuring the molecular gas mass through molecular line spectroscopy is time consuming, but an alternative way to estimate the gas mass of a galaxy is to derive the dust mass first based on the FIR/submm continuum data, then apply a conversion using the 'dust-to-gas ratio'. Assuming that the dust production mechanism is mainly governed by stars, i.e., through AGB stars and supernovae, one would expect that the dust properties are related to the metallicity of galaxies, resulting the dust-to-metal ratio is described as a function of metallicity (Mattsson et al. 2014). Observations of local star-forming galaxies have showed that there exists a linear correlation between the dust-to-gas ratio and the gas-phase metallicity (e.g., Draine et al. 2007; Kahre et al. 2018), though there may be deviations from the trend for the lowest metallicity galaxies (e.g., Remy-Ruyer et al. 2014; De Vis et al. 2019). Such scaling relations should be taken into consideration when modelling the evolution of dust in galaxies, and yet they are still not completely reproduced by the model (e.g., Hou et al. 2019; Li et al. 2019). Gas-phase metallicity is the most critical parameter for determining the dust-to-gas ratio and dust-to-metal ratio (Popping et al. 2017; Li et al. 2019), but the model has not been statistically tested for high-z galaxies. Observations of DLA and GRB absorbers at $z = 2$–4 argued that there is little variation in dust-to-metal ratio for more than an order of magnitude in the metallicity (De Cia et al. 2013, 2016; Wiseman et al. 2017), which is completely different from the model predictions. Therefore, in order to constrain dust scaling relations at high-z, we need a large sample of galaxies with dust and metallicity information at $z > 2$.

The NEP region, the only *Euclid*-deep field in the northern hemisphere, is the most appropriate field to perform such studies, since we will be able to use 0.92-1.85 μm spectra where the [OII] and [OIII] lines of $1 < z < 2$ galaxies are redshifted into. At line flux limits of $7 \times 10^{-17}\,\mathrm{erg\,s^{-1}\,cm^{-2}}$ and with broad-band observations down to 26 AB mag in YJH-filters, 8×10^5 galaxies at $1 < z < 2$ will be available in this $\sim 10\,\mathrm{deg}^2$ field that will statistically constrain the fundamental mass-metallicity relation (comparable to the entire SDSS local galaxy sample). Combining the gas-phase metallicities measured by the near-IR spectroscopy with the dust mass, we expect to constrain dust scaling relation in disk galaxies at $z > 1$ for the first time.

The scheduled TolTEC survey will provide 1.1, 1.4, and 2 mm continuum maps over the *Euclid*-deep field area. The multi-color 1.1 to 2 mm data points down to 0.26 mJy rms will be used to calculate infrared luminosities above of galaxies with $L_{IR} > 5 \times 10^{12}\,L_\odot$ at $z \sim 2$, roughly equivalent to dust masses of $6 \times 10^7\,M_\odot$. However, the estimated dust mass significantly depends on the emission opacity and the dust temperature, which should be more clearly constrained by the photometry shortward and longward the wavelength of peak emission. Adding SCUBA-2 850 μm to TolTEC mm data will reduce the uncertainties in T_{dust}, playing a key role in the estimation of dust mass and thus dust scaling relations at $z > 1$.

Key Science 3: Star Formation and AGN Activity

Like in the case of cosmic star-formation history, AGN activity has been decreasing since $z > 2$–3, suggesting that the decline of star formation is related to the evolution of gas accretion and outflows driven by AGN (e.g., Wall, Pope & Scott 2008). The maximum growth of supermassive black holes occurs in the

accretion phase; therefore we need a complete census of the AGN population at the time of the peak in star formation in order to understand the role of AGN in regulating star formation, including the most heavily obscured sources. X-ray emission at energies higher than 10 keV (to penetrate the obscuring matter) is the best tool to probe obscured AGN based on the low L_X/L_{IR} ratio – but this can also be done in the submm. There is therefore a natural synergy here between FIR/submm surveys and X-ray surveys.

The X-ray telescope *eROSITA* was successfully launched in July 2019, with the goal of carrying out an all-sky survey in the 0.3–10 keV bands. Within the all-sky survey, $\sim 150\,\mathrm{deg}^2$ around the NEP will be visited most frequently, to allow > 10 ks exposure time in total. The 5σ detection limit is expected to be $3 \times 10^{-15}\,\mathrm{erg\,s^{-1}\,cm^{-2}}$ in the soft X-ray bands (0.5–2 keV) and $6 \times 10^{-14}\,\mathrm{erg\,s^{-1}\,cm^{-2}}$ in the hard bands (2–10 keV), $\times 3$ times deeper than that of the all-sky survey. Detection of AGN can become extremely challenging when absorption reaches the Compton-thick level; thus Compton-thick AGNs are thought to be very rare, with a number density of $2.6 \times 10^{-4}\,\mathrm{Mpc^{-3}}$ (Daddi et al. 2007, but highly uncertain, since it is only based on data from very small fields). In order to select "obscured" AGN based on criteria such as $L_{IR,AGN}/L_X > 20$ (e.g., Chang et al. 2017) or "Compton-thick" AGN ($L_{IR,AGN}/L_X \sim 80$; Fiore et al. 2009), we need an FIR/submm survey that has a flux limit appropriate for detecting $L_{IR} > 10^{12}\,\mathrm{L_\odot}$ galaxies. The AGN-dominated IR luminosity is typically derived from the mid-IR (e.g., 6 μm) luminosity, but FIR continuum photometry is critical for breaking the SF/AGN degeneracy in these systems.

Besides the study of newly found, rare obscured AGN, we already have a large sample of AGN over the NEP field, particularly those selected at radio wavelengths using 1.4 and 0.6 GHz data. The 850-μm continuum flux from the SCUBA-2 NEP survey is particularly useful in improving the SED modeling by: (i) constraining the drop-off of the cold-dust emission spectrum; (ii) making a more robust cross-matching between far-IR and mid-IR/optical counterparts; and (iii) including physically motivated modelling of the stellar component of these sources. Through this process, we will be able to investigate how the specific star-formation rate varies as a function of radio jet power (e.g., Karouzos et al. 2014), which shows the effectiveness of AGN feedback to the star formation process.

Other Science Topics: Multi-wavelength Power of the NEP field

While the above three key science themes assume a combination of SCUBA-2 850-μm data with the data from TolTEC 1.1 mm (expected to be available as early as 2021, since the commissioning of TolTEC will be in 2020), *Euclid*-Deep (expected to be available as early as 2023 with the launch date being 2022), and *eROSITA* (expected to be available as early as 2020), we list numerous science topics that are already in progress with the existing multi-wavelength data sets over the NEP using the 850-μm data obtained already. The 850-μm data plays a decisive role in each topic by providing a tracer of attenuation-free star formation for galaxies at low- and high-z. The completion of M17BL007 will increase the statistics of the submm galaxy population and associated structures around it (e.g., proto-clusters) and push down the flux limits that can be probed by a factor of > 10, by stacking studies.

Galaxy Clusters and Other Structures The reversal of the star formation–density relation (i.e., the spatially averaged SFR of galaxies decreases with local density at low redshifts, but increases with local density at high redshifts) occurs at $z \sim 1$ for field galaxies and is expected to occur at higher redshifts for cluster galaxies because of additional cluster-driven quenching mechanisms. In other words, the activity of galaxies is quenched earlier in cluster environments; however, observations show diverse results about the star formation in galaxies resided in high-z cluster environment (e.g. Brodwin et al. 2013; Alberts et al. 2016). We therefore need to tackle this issue with an unbiased view of the star formation activity and a larger sample of galaxy clusters at high redshifts.

The power of JCMT SCUBA-2 850-μm data (combined with other multi-wavelength data) comes from the fact that it can provide an unbiased view of star-formation activity at high redshift ($z \sim 2$), especially for central regions in galaxy groups and clusters. We can study the star-formation and nuclear activity of central galaxies in galaxy groups/clusters by comparing with that of field galaxies and with cluster galaxies at different redshifts. *Because the mean separation of massive galaxy clusters is about $50\,h^{-1}$ Mpc, it is necessary to complete the ~ 4 deg^2 area for the AKARI wide field in order to obtain a statistically meaningful sample of clusters (e.g., 50 h^{-1} Mpc corresponds to 0.8° at $z = 2$).* By comparing the results from this field with

those from other fields with similar data sets (e.g. S2COSMOS), we can also study the effects of cosmic variance (e.g. Geller et al. 2016).

Cosmic Star-Formation History Star-forming galaxies selected in the rest-frame UV or optical comprise the bulk of the star-forming galaxy population, with SFRs much lower than those of DSFGs. Nevertheless, how much SFR is hidden by dust in these typical star-forming galaxies should be investigated by estimating their dust attenuation, which is best determined through the comparison between rest-frame UV/optical and rest-frame IR. In general, stacking analyses are adopted to estimate the average flux density in IR bands (e.g., Carilli et al. 2008; Coppin et al. 2015; Alvarez-Marquez et al. 2016) to probe below the detection limit.

850 μm spatial resolution is better than that of *Herschel*/SPIRE by a factor of > 2, making stacking analyses much more reliable. For example from the S2CLS 850 μm data covering the central $\sim 0.6\,\mathrm{deg}^2$, we applied stacking to ~ 560 EROs (Extremely Red Objects selected by $R - K_\mathrm{s} > 5.5$; Seo et al. 2019) to find an upper limit of 0.3 mJy. Unfortunately the numbers of EROs and other optical/nearIR-selected galaxy populations *within the existing S2CLS 850 μm coverage* is of order of few hundreds, insufficient to explore infrared properties of optical/nearIR-selected galaxies among different subgroups of galaxies in terms of stellar mass and evolutionary stages (such as star-forming and passively evolving). The completion of the M17BL007 is therefore important since we are going to have a few times more coverage that would enable us to estimate average far-IR flux density from galaxies that share similar physical quantities. We already have optically selected star-forming galaxy samples defined at $z = 0.4$, 0.8, and 1.47 (from the Subaru/HSC narrow-band surveys), and at $1 < z < 2$ and $z > 3$ (from the Subaru/HSC broad-band surveys combined with near-IR observations). *By extending the 850-μm coverage to the full $\sim 4\,\mathrm{deg}^2$, it will be possible to investigate how much attenuation is hindering the SFRs of typical galaxies, as well as the factors governing such attenuation.*

With the upcoming TolTEC data, which will have a factor of 3 better spatial resolution than SCUBA-2 at 850 μm (i.e., 5 arcsec for TolTEC 1.1 mm and 14 arcsec for SCUBA-2 850 μm), deconvolved 850-μm images can be used to remove biases for estimating the average total IR luminosity based on the available monochromatic photometry (Serjeant 2019; Fig. 2).

PAH-to-FIR Ratio for Local Starbursts The characteristics of infrared SEDs of galaxies arises from the combination of the emissions from Polycyclic Aromatic Hydrocarbon (PAH) molecules (or hot/small dust grains) in the mid-IR and the thermal radiation of large grains in the equilibrium temperatures that peaks at the far-IR wavelengths. PAH molecules are believed to be located in the photo-dissociation regions, the interface between the ionized and molecular interstellar medium (Bakes & Tielens 1998), while the far-IR dust continuum is from the entire dust clouds or from dust in the diffuse ISM. This suggests using the ratio between PAH emission and dust continuum as a proxy to probe the geometry of star-forming regions. This is effectively being done using the IR8= $L_{IR}/L_{8\mu m}$ ratio as a tracer of compactness in distant star-forming galaxies (Elbaz et al. 2011). The quantity IR8 increases as a galaxy produces more stars compared to galaxies on the star-forming main sequence (in other words, the total IR luminosity increases; Murata et al. 2014; Kim et al. 2019), suggesting that the star formation in such galaxies (above the main sequence) occurs in a different way – probably with higher efficiency and in more compact volumes. For these reasons, IR8 is one of the key parameters for describing the dust SEDs of galaxies (Schreiber et al. 2018).

In the local Universe where we have highly reliable photometric redshifts, *combining 850 μm with 250, 350, and 500 μm data reduces uncertainties in dust temperature determinations and provides reliable estimates of the total infrared luminosity.* The variation of IR8 in terms of specific SFR for local main sequence galaxies will be used to estimate total IR luminosity of galaxies without far-IR detections. However, since unexpectedly large amount of cold dust in the diffuse ISM can increase the total IR luminosity compared to PAH emission (e.g., recently quenched galaxies), which can also result in higher IR8, more accurate constraints on dust emission by sub-mm data would be necessary to understand the connection between the actual star-formation activity and dust components.

References

• Alberts, S., Pope, A., Brodwin, M., et al. 2016, ApJ, 825, 72 • Alvarez-Marquez, J., Burgarella, D., Heinis, S., et al. 2016, A&A, 587, 122 • Bakes, E. L. O., & Tielens, A. G. G. M., 1998, ApJ, 499, 258 • Behrens, C., Pallotini, A., Ferrara, A., et al. 2018, MNRAS, 477, 552 • Bouwens, R. J., Aravena, M., Decarli, R., et al. 2016, ApJ, 833, 72 • Bouwens, R. J., Oesch, P. A., Illingworth, G. D., et al. 2017, ApJ, 843, 129 • Bowler, R. A. A., Bourne, N., Dunlop, J. S., et al. 2018, MNRAS, 481, 1631 • Brodwin, M., Stanford, S. A., Gonzalez, A. H., et al. 2013, ApJ, 779, 138 • Cai, Z.-Y., Lapi, A., Xia, J.-Q., et al. 2013, ApJ, 768, 21 • Carniani, S., Maiolino, R., Smit, R., et al. 2018, ApJL, 854, 7 • Carilli, C. L., Lee, N., Capak, P., et al. 2008, ApJ, 689, 883 • Casey, C. M., Narayana, D., Cooray, A., 2014, Physics Reports, 541, 45 • Casey, C. M., Zavala, J. A., Spilker, J., et al. 2018, ApJ, 862, 77 • Chang, Y.-Y., Le Floc'h, E., Juneau, S., et al. 2017, ApJS, 233, 19 • Coppin, K. E. K., Geach, J. E., Almani, O., et al. 2015, MNRAS, 446, 1293 • da Cunha, E., Walter, F., Smail, I. R., et al. 2015, ApJ, 806, 110 • Daddi, E., Alexander, D. M., Dickinson, M., et al. 2007, ApJ, 670, 173 • De Cia, A., Ledoux, C., Savaglio, S., et al. 2013, A&A, 560, 88 • De Cia, A., Ledoux, C., Mattsson, L., et al. 2016, A&A, 596, 97 • De Vis, P., Jones, A., Viaene, S., et al. 2019, A&A, 623, 5 • Draine, B. T., Dale, D. A., Bendo, G., et al. 2007, ApJ, 663, 866 • Elbaz, D., Dickinson, M., Hwang, H. S., et al. 2011, A&A, 533, 119 • Fiore, F., Puccetti, S., Brusa, M., et al. 2009, ApJ, 693, 447 • Geach, J. E., Dunlop, J. S., Halpern, M., et al. 2017, MNRAS, 465, 1789 • Geller, M. J., Hwang, H. S., Dell'Antonio, I. P., et al. 2016, ApJS, 224, 11 • Hodge, J. A., Karim, A., Smail, I., et al. 2013, ApJ, 768, 91 • Hou, K.-C., Aoyama, S., Hirashita, H., et al. 2019, MNRAS, 485, 1727 • Inoue, A. K., Tamura, Y., Matsuo, H., et al. 2016, Science, 352, 1559 • Kahre, L., Walterbos, R. A., Kim, H., et al. 2018, ApJ, 855, 133 • Karouzos, M., Im, M., Trichas, M., et al. 2014, ApJ, 784, 137 • Kim, S. J., Lee, H. M., Matsuhara, H., et al. 2012, A&A,, 548, 29 • Kim, S. J., Jeong, W.-S., Goto, T., et al. 2019, PASJ, 71, 11 • Laporte, N., Ellis, R. S., Boone, F., et al. 2017, ApJL, 837, 21 • Le Floc'h, E., Papovich, C., Dole, H., et al. 2005, ApJ, 632, 169 • Lesniewska, A. & Michalowski, M. J. 2019, A&A, 624, 13 • Li, Q., Narayana, D., Dave, R., 2019, arXiv: 1906.09277 • Liang, L., Feldmann, R., Keres, D., et al. 2019, arXiv: 1902.10727 • Magnelli, B., Popesso, P., Berta, S., et al. 2013, A&A, 553, 132 • Matsuhara, H., Wada, T., Matsuura, S., et al. 2006, PASJ, 58, 673 • Mattsson, L., De Cia, A., Andersen, A. C., et al. 2014, MNRAS, 440, 1562 • Murata, K., Matsuhara, H., Inami, H., et al. 2014, A&A, 566, 136 • Nayyeri, H., Ghotbi, N., Cooray, A., et al. 2018, ApJS, 234, 38 • Oi, N., Matsuhara, H., Murata, K., et al. 2014, A&A, 566, 60 • Pallottini, A., Ferrara, A., Decataldo, D., et al. 2019, MNRAS, 487, 1689 • Patel, H., Clements, D. L., Vaccari, M., et al. 2013, MNRAS, 428, 291 • Popping, G., Somerville, R. S., Galametz, M. 2017, MNRAS, 471, 3152 • Remy-Ruyer, A., Madden, S. C., Galliano, F., et al. 2014, A&A, 563, 31 • Schreiber, C., Elbaz, D., Pannell, M., et al. 2018, A&A, 609, 30 • Seo, H., Jeong, W.-S., Kim, M., et al. 2018, JKAS, 51, 49 • Seo, H., Jeong, W.-S., Shim, H., et al. 2019, PASJ, *in press* • Serjeant, S. 2019, RNAAS, *accepted* • Smit, R., Bouwens, R. J., Carniani, S., et al. 2018, Nature, 553, 178 • Takagi, T., Matsuhara, H., Goto, T., et al. 2012, A&A, 537, 24 • Tamura, Y., Mawatari, K., Hashimoto, T., et al., 2019, ApJ, 874, 27 • Wall, J.V., Pope A., Scott, D., 2008, MNRAS, 383, 435 • Wang, W.-H., Lin, W-C., Lim, C.-G., et al., 2017, ApJ, 850, 37 • Watson, D., Christensen, L., Knudsen, K. K., et al. 2015, Nature, 519, 327 • Whitaker, K. E., Pope, A., Cybulski, R., et al. 2017, ApJ, 850, 208 • White, G. J., Pearson, C., Braun, R., et al. 2010, A&A, 517, 54 • Willott, C. J., Carilli, C. L., Wagg, J., et al. 2015, ApJ, 807, 180 • Wiseman, P., Schady, P., Bolmer, J., et al. 2017, A&A, 599, 24 • Zavala, J. A., Montana, A., Hughes, D. H., et al. 2018, Nature AStronomy, 2, 56

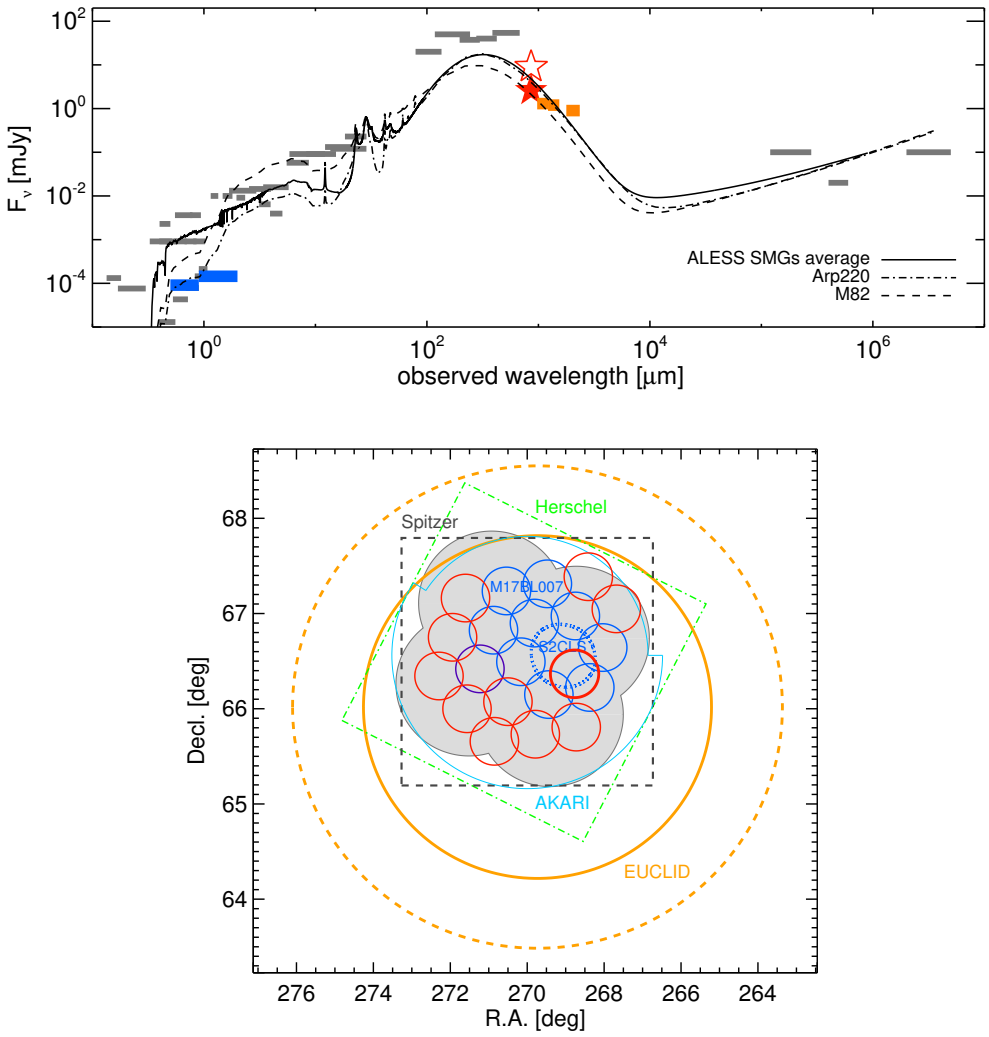

Figure 1: **(Top)** 5-σ detection limits of the existing surveys in the NEP region (gray lines), planned *Euclid*-deep survey (blue lines), TolTEC survey (orange lines), as well as the shallow (open star) and the proposed deep (filled star) SCUBA-2 850 μm survey. Overplotted are some SED templates: the average of ALESS submillimeter galaxies (da Cunha et al. 2015); Arp 220; and M82. All templates are redshifted to $z = 2.7$, which is a median redshift of ALESS submillimeter galaxies, and scaled to represent $L_{IR} = 5 \times 10^{12}\,L_\odot$. Note that the *Herschel*-PACS and SPIRE data over 100–500 μm are not deep enough to detect ULIRGs at $z > 2$; on the other hand, 850 μm can be used to select such galaxies. The depth of the *Euclid*-deep field matches with the proposed survey depth by TolTEC, yet the TolTEC colors are not the best placed to constrain dust temperatures for $z \sim 3$ galaxies, since the SED drops rapidly at > 2 mm. Therefore the addition of an 850-μm data point at comparable depth to TolTEC is critical for constraining dust temperatures of DSFGs in the early Universe, breaking the T_{dust}–z degeneracy. **(Bottom)** The areal coverages of the existing and planned surveys in the NEP region. Shaded clover-shaped area represents Subaru HSC *grizy* imaging survey (Oi et al., *in preparation*). *AKARI* NEP-wide (Kim et al. 2012), *Spitzer* 3.6/4.5 μm (Nayyeri et al. 2018), *Herschel* SPIRE 250/350/500 μm, and upcoming *EUCLID* field is compared with the 850 μm coverage obtained from S2CLS (blue dotted line; Geach et al. 2017) and M17BL007 (blue solid line). To complete 850 μm map over the entire $\sim 4\,\mathrm{deg}^2$ covered by *AKARI*, *Spitzer*, and *Herschel*, we need additional 10 PONG1800 pointings (marked as red). In the deepest region (thick red line), we propose to obtain deeper (~ 0.8 mJy rms) 850 μm data in order to push down below the confusion limit and achieve sensitivity matching to that of TolTEC 1.1 mm data.

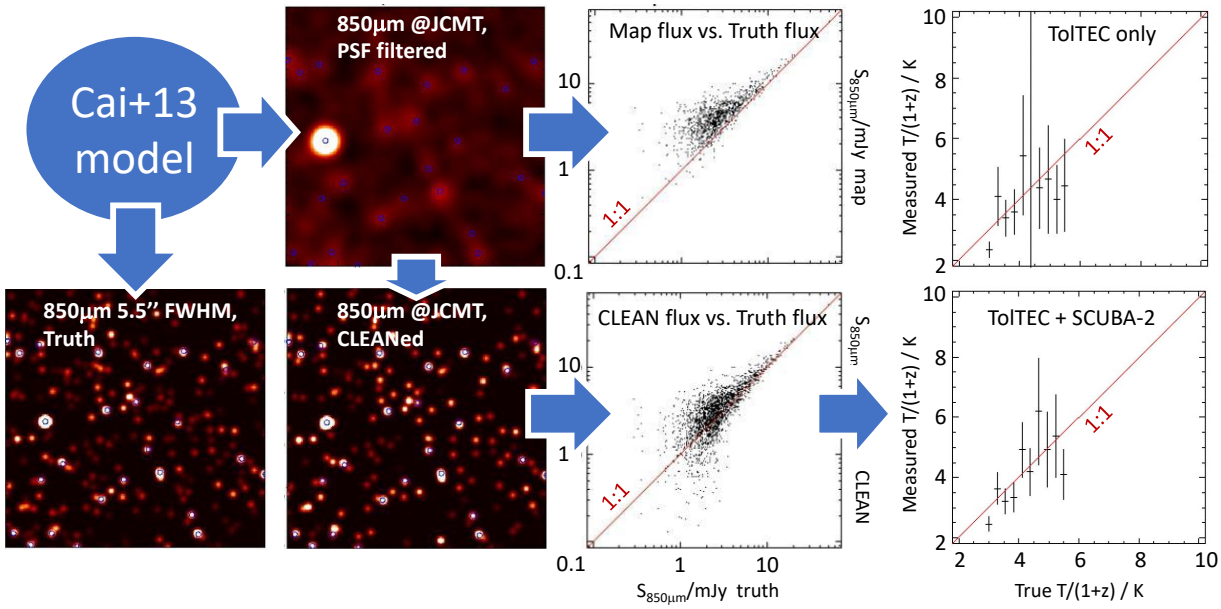

Figure 2: Schematic of our CLEAN deconvolution procedure, from Serjeant 2019 (RNAAS in press). We use the Cai+13 model in a PONG1800 area, 250 arsec^2 segments of which are shown. We simulate the 1.1-mm population to 0.1 mJy, including its redshift distribution, and combine this with a starburst SED to create an 850-μm population. We create a simulation at JCMT resolution, shown here point-source-filtered with added noise, and a truth image at LMT resolution. We make a CLEAN deconvolution using the underlying 1.1-mm positions as a prior as appropriate, e.g., for MIPS/AKARI/JVLA cross-IDs. **Note the striking visual correspondence with the truth image.** Blue circles mark the locations of 1.1-mm sources extracted from simulated TolTEC LSS survey point-source-filtered images. Fluxes measured from the CLEANed map have $\sim \times 1.5$ less uncertainty than the simple PSF-convolved map, and Eddington bias is mitigated. Finally, we show that the combination of TolTEC LSS data with SCUBA-2 can constrain cold colour temperatures, while TolTEC on its own has no discriminatory power.